

Finite Size Analysis of the Structure Factors in the Antiferromagnetic XXZ Model

M. Karbach, K.-H. Mütter* and M. Schmidt
Physics Department, University of Wuppertal
42097 Wuppertal, Germany
 (23.02.94)

We perform a finite size analysis of the longitudinal and transverse structure factors $S_j(p, \gamma, N)$, $j = 1, 3$ in the groundstate of the spin- $\frac{1}{2}$ XXZ model. Comparison with the exact results of Tonegawa for the XX model yields excellent agreement. Comparison with the conjecture of Müller, Thomas, Puga and Beck reveals discrepancies in the momentum dependence of the longitudinal structure factors.

PACS number: 75.10 -b

I. INTRODUCTION

In a previous publication,¹ two of us (M.K. and K.-H.M.) have studied the structure factor $S(p, N)$ in the groundstate of the antiferromagnetic Heisenberg (AFH)-model on finite rings with $N = 4 - 30$ sites. We found that finite size effects die out with N^{-2} and with a coefficient $c(p)$ increasing with momentum p . The “gross”-structure of $S(p, N)$ is well described by $-\ln(1-p/\pi)$ for all values $p < \pi$. Therefore indications for a critical behavior in the limit $p \rightarrow \pi$ can be seen already for all values of p . For this reason the structure factor appears to be more suited than the spin-spin correlators to extract the critical behavior from finite systems.

In the present paper we are going to extend this analysis to the XXZ-model with Hamiltonian:

$$H = 2 \sum_{x=1}^N [S_1(x)S_1(x+1) + S_2(x)S_2(x+1) + \cos \gamma S_3(x)S_3(x+1)], \quad (1.1)$$

which coincides with the AFH-Hamiltonian in the isotropic limit $\gamma = 0$. The groundstate properties of the spin-spin correlators at large distances $x \rightarrow \infty$ and in the critical regime $0 \leq \gamma \leq \pi/2$ have been found by Luther and Peschel²

$$\langle 0 | S_j(0) S_j(x) | 0 \rangle \xrightarrow{x \rightarrow \infty} \frac{(-1)^x}{x^{\eta_j}}, \quad j = 1, 3, \quad (1.2)$$

with critical exponents:

$$\eta_1 = \eta_3^{-1} = 1 - \frac{\gamma}{\pi}, \quad \text{for } 0 \leq \gamma \leq \frac{\pi}{2}. \quad (1.3)$$

The critical exponent η_3 were derived also from the quantum inverse scattering method.³ Both exponents η_1 and η_3 are also predicted by conformal invariance.⁴

The structure factors are defined as the Fourier transforms of the longitudinal and transverse spin-spin correlators:

$$S_j(p = 2\pi k/N, \gamma, N) = 1 + (-1)^k 4 \cdot \langle 0 | S_j(0) S_j(N/2) | 0 \rangle + 8 \cdot \sum_{x=1}^{N/2-1} \langle 0 | S_j(0) S_j(x) | 0 \rangle \cdot \cos(px), \quad j = 1, 3. \quad (1.4)$$

The large distance properties of the spin-spin correlators (1.2) induce a specific behavior of the corresponding structure factors for momenta $p \rightarrow \pi$:

$$S_j(p, \gamma) = a_j + b_j \cdot \left(1 - \frac{p}{\pi}\right)^{\eta_j - 1} \quad \text{for } j = 1, 3 \quad \text{and} \quad 0 < \gamma \leq \frac{\pi}{2}, \quad (1.5)$$

where the critical exponents η_j , $j = 1, 3$ are given by (1.3). Note that the longitudinal structure factor stays finite for $p = \pi$ and $0 < \gamma \leq \pi/2$, whereas the transverse structure factor diverges. The questions we address here are the following:

- (1) Is it possible to see the specific behavior (1.5) already on finite systems?

- (2) Is rotation invariance in spin space restored in the isotropic limit $\gamma \rightarrow 0, \eta_j \rightarrow 1$?
- (3) What is the leading singularity of $S_j(p, \gamma = 0, N = \infty)$ for $p \rightarrow \pi$?
- (4) What is the leading large N behavior of the structure factors $S_j(p = \pi, \gamma, N)$ in the isotropic limit $\gamma \rightarrow 0$?

The answer to the second question is of special interest in view of the results of Singh, Fisher and Shankar.⁶ Following Ref. 6, the transverse and longitudinal structure factors $S_j(p = \pi, \gamma', N = \infty), j = 1, 3$ behave differently if we approach the isotropic limit from the noncritical regime $\cos \gamma = \cosh \gamma' > 1$:

$$S_j(p = \pi, \gamma', N = \infty) \rightarrow \gamma'^{-\lambda_j}, \quad (1.6)$$

where

$$\lambda_1 = 1.5, \quad \lambda_3 = 2. \quad (1.7)$$

It is well known⁵ that in the noncritical regime $\gamma' > 0$ the large distance behavior of the correlators is governed by a finite correlation length:

$$\xi(\gamma') \xrightarrow{\gamma' \rightarrow 0} \frac{1}{8} \exp\left(\frac{\pi^2}{2\gamma'}\right), \quad (1.8)$$

which diverges exponentially for $\gamma' \rightarrow 0$. Therefore, both longitudinal and transverse structure factors stay finite at $p = \pi, \gamma' \neq 0$. In order to see the effect of the divergencies (1.6) and (1.7) on finite rings, one could think of a finite size scaling ansatz of the structure factors:

$$S_j(p = \pi, \gamma', N) = S_j(p = \pi, \gamma', N = \infty) \cdot g_j(z), \quad (1.9)$$

in the combined limit

$$N \rightarrow \infty, \quad \gamma' \rightarrow 0, \quad z = \frac{N}{\xi(\gamma')} \text{ fixed.} \quad (1.10)$$

Note, however, that the correlation length increases exponentially in the limit $\gamma' \rightarrow 0$. Therefore, extremely large systems are needed, to extract the structure factors $S_j(p = \pi, \gamma', N = \infty)$ close to the isotropic limit. Having this in mind, we did not make an attempt, to see the effect of the divergencies (1.6) on our rings with $N \leq 28$ sites.

The outline of the paper is as follows. In Sec. II we demonstrate, that the longitudinal and transverse structure factors obey approximate scaling laws for all momentum values $0 < p < \pi$ and γ -values $0 \leq \gamma \leq \pi/2$. In Sec. III, we perform a finite size analysis of the structure factors for noncritical momenta $p \leq 6\pi/7$. In Sec. IV we study how the transverse and longitudinal structure factors at $p = \pi$, converge to each other in the limit $\gamma \rightarrow 0$. Finally, we propose in Sec. V a finite size scaling ansatz with an appropriate scaling variable, which accounts for all finite size effects at noncritical momenta $p < \pi$ and at the critical momentum $p = \pi$.

II. APPROXIMATE SCALING PROPERTIES OF THE LONGITUDINAL AND TRANSVERSE STRUCTURE FACTORS

In Fig. 1 we have plotted the longitudinal structure factor $S_3(p, \gamma, N)$ on finite rings with $N = 4, 6, \dots, 28$ sites and $\gamma/\pi = 0, 0.1, 0.2, 0.3, 0.4, 0.5$ as function of the ‘‘scaling variable’’:

$$L_3(p, \gamma) = \frac{\eta_3}{\eta_3 - 1} \left[1 - \left(1 - \frac{p}{\pi} \right)^{\eta_3 - 1} \right]. \quad (2.1)$$

The normalization in the scaling variable (2.1) has been chosen such that the limit to the isotropic case $\eta_3 \rightarrow 1$ can be performed:

$$L_3(p, \gamma)|_{\gamma=0} = -\ln \left(1 - \frac{p}{\pi} \right). \quad (2.2)$$

Indeed (2.2) has been found in Ref. 1 as the adequate variable in the isotropic case. Looking at Fig. 1, we observe that all data points follow approximately a single straight line with slope one as long as $p < \pi$. For these momentum

values finite size effects appear to be small in contrast to the “critical” point $p = \pi$, where finite size effects are large. Deviations from the straight line in Fig. 1 and finite size effects become visible in Fig. 2 where we have plotted the difference:

$$\Delta_3(p, \gamma, N) = S_3(p, \gamma, N) - L_3(p, \gamma), \quad (2.3)$$

versus the scaling variable (2.1). Note the surprising behavior of the longitudinal structure factor of the XX-model:

$$S_3(p, \gamma = \pi/2, N) = L_3(p, \gamma = \pi/2) = \frac{2}{\pi} p. \quad (2.4)$$

It is free of any finite size effect! This is proven in Appendix A using the rigorous results of Lieb, Schultz and Mattis.⁸ For decreasing values of γ we observe in the differences (2.3) a “fine” structure with a minimum for larger p -values. Moreover, there seems to be a maximum for small p and γ values.

Let us now turn to the transverse structure factor $S_1(p, \gamma, N)$ which we present in Fig. 3 as function of the analogous “transverse scaling variable”:

$$L_1(p, \gamma) = \frac{\eta_1}{\eta_1 - 1} \left[1 - \left(1 - \frac{p}{\pi} \right)^{\eta_1 - 1} \right]. \quad (2.5)$$

Both variables (2.1) and (2.5) coincide in the isotropic limit (2.2). Again we observe an approximate scaling, which however is less impressiv than the scaling of the longitudinal structure factor. In order to resolve detailed features and finite size effects we plot again in Fig. 4 the difference:

$$\Delta_1(p, \gamma, N) = S_1(p, \gamma, N) - L_1(p, \gamma), \quad (2.6)$$

as function of L_1 . A comparison of Figs. 2 and 4 reveals two important differences in the finite size effects of the longitudinal and transverse structure factors S_3 and S_1 :

- (1) They are zero in $S_3(p, \gamma = \pi/2, N)$, but nonzero in $S_1(p, \gamma = \pi/2, N)$.
- (2) They are small in S_3 but large in S_1 for small momentum values.

III. FINITE SIZE ANALYSIS OF THE STRUCTURE FACTORS FOR NONCRITICAL MOMENTA

We have analyzed the finite size dependence of the structure factors for fixed momenta:

$$p = \begin{cases} \frac{\pi}{4}, \frac{3\pi}{4} & \text{for } N = 8, 16, 24 \\ \frac{\pi}{3}, \frac{2\pi}{3} & \text{for } N = 6, 12, 18, 24 \\ \frac{\pi}{2} & \text{for } N = 4, 8, 12, 16, 20, 24, 28, \end{cases}$$

which can be realized on the systems with size N given above. The N -dependence of the differences (2.3) and (2.6) can be parametrized by:

$$\Delta_j(p, \gamma, N) = \Delta_j(p, \gamma) + \frac{c_j(p, \gamma)}{N^2}, \quad j = 1, 3. \quad (3.1)$$

As an example we show in Figs. 5(a) and 5(b) the finite size effects of the structure factors at:

$$p = \frac{\pi}{2} \text{ and } \frac{\gamma}{\pi} = 0, 0.1, 0.2, 0.3, 0.4, 0.5.$$

The slopes $c_j(p, \gamma)$ turn out to be small for small momentum values $p < \pi/2$ and increase rapidly for $p \rightarrow \pi$. Indeed there seems to be a singularity of the type $(1 - p/\pi)^{\eta_j - 3}$. Therefore we have plotted in Fig. 6 the slopes versus the variable:

$$\frac{\eta_j(\eta_j - 2)}{2} \left[1 - \left(1 - \frac{p}{\pi} \right)^{\eta_j - 3} \right]. \quad (3.2)$$

We observe an almost linear behavior in this variable. Note that Fig. 6 allows us to compare the finite size effects (3.1) of the longitudinal and transverse structure factors: They coincide in the isotropic limit but differ more and

more with increasing γ . A motivation for the special choice of the variable (3.2) is given in the Sec. V. In Fig. 6 we have included as well the momenta:

$$p = \begin{cases} \frac{\pi}{5}, \frac{2\pi}{5}, \frac{3\pi}{5}, \frac{4\pi}{5} & \text{for } N = 10, 20 \\ \frac{\pi}{6}, \frac{5\pi}{6} & \text{for } N = 12, 24 \\ \frac{\pi}{7}, \frac{2\pi}{7}, \frac{3\pi}{7}, \frac{4\pi}{7}, \frac{5\pi}{7}, \frac{6\pi}{7} & \text{for } N = 14, 28, \end{cases}$$

which occur on two systems. Here we have assumed that the finite size dependence is described correctly by (3.1). Our estimates for the structure factors in the thermodynamical limit can be seen from the solid dots and squares in Figs. 7(a)-(f).

So far our estimate of the thermodynamical limit is restricted to momentum values $p \leq 6\pi/7$ due to the finiteness of our systems $N \leq 28$. Additional information on the structure factors for p -values:

$$p = \pi \left(1 - \frac{2}{N} \right), \quad N = 14, 16, \dots, 28, \quad (3.3)$$

close to the ‘‘critical’’ momentum $p = \pi$ can be obtained, if finite size scaling holds for the structure factors

$$S_j(p, \gamma, N) = S_j(p, \gamma, N = \infty) \cdot g_j(z, \gamma), \quad (3.4)$$

in the combined limit

$$N \rightarrow \infty, \quad p \rightarrow \pi, \quad z = \left(1 - \frac{p}{\pi} \right) N \quad \text{fixed}. \quad (3.5)$$

Note, that the scaling variable z is just 2 for the momenta listed in (3.3). The scaling function at this value can be taken from:

$$g_j(2, \gamma) = \frac{S_j(p = 6\pi/7, \gamma, N = 14)}{S_j(p = 6\pi/7, \gamma, N = \infty)}, \quad (3.6)$$

and is shown as function of γ in Fig. 8. In this way we get from the finite size scaling ansatz (3.4) an estimate of the thermodynamical limit of the structure factors:

$$S_j(p = \pi(1 - 2/N), \gamma, \infty) = \frac{S_j(p = \pi(1 - 2/N), \gamma, N)}{g_j(2, \gamma)} \quad (3.7)$$

for the momenta listed in (3.3). The result for the differences (2.3) and (2.6) is marked in Figs. 7(a)-(f) by the open dots and squares.

The validity of our finite size approach to the structure factors in the thermodynamical limit can be tested in case of the XX model ($\gamma = \pi/2$), where the transverse structure factor is known exactly from the results of Toneyawa.⁹

The dotted curve in Fig. 7(a) represents the exact result; the solid and open squares the results of our finite size analysis.

In Ref. 10 Müller *et al.* have made a conjecture on the dynamical correlation functions in the XXZ model. From this conjecture one gets a prediction on the static structure factors $S_1(p, \gamma)$, $S_3(p, \gamma)$, which we have plotted in Figs. 7(a)-(f) by the dashed and solid curves, respectively. We observe:

- (1) Excellent agreement of our finite size analysis with the exact result of Ref. 9 for $\gamma = \pi/2$. The conjecture of Müller¹⁰ *et al.* for the transverse structure factor is systematically above the exact result.
- (2) The conjecture of Müller¹⁰ *et al.* for the transverse structure factor at $\gamma/\pi = 0.4, 0.3, 0.2, 0.1, 0$ deviates from our finite size analysis more and more, if the momentum increases and if γ decreases.
- (3) The conjecture of Müller¹⁰ *et al.* for the longitudinal structure factor at $\gamma/\pi = 0.4, 0.3, 0.2, 0.1, 0$ is in striking disagreement from our finite size analysis. In particular, the minimum we find in the difference $\Delta_3(p, \gamma) = S_3(p, \gamma) - L_3(p, \gamma)$ at momentum $p = p(\gamma)$ listed in TABLE I:

TABLE I. The position $p = p(\gamma)$ of the minimum of $\Delta_3(p, \gamma)$ as a function of $p(\gamma)$.

γ/π	0.4	0.3	0.2	0.1	0
$p(\gamma)/\pi$	0.51	0.59	0.66	0.73	0.82

is not predicted by the conjecture of Ref. 10. Beyond the minimum our finite size analysis yields an increase of the difference (2.3) which might be linear or even stronger in the scaling variable $L_3(p, \gamma)$ [cf.(2.1)]. A linear extrapolation for the structure factor in the isotropic case yields:

$$\Delta_3(p, \gamma = 0) = S_3(p, \gamma = 0) + \ln \left(1 - \frac{p}{\pi}\right) = -A \cdot \ln \left(1 - \frac{p}{\pi}\right) \quad \text{for } p \rightarrow \pi, \quad (3.8)$$

where

$$A \gtrsim 0.12. \quad (3.9)$$

We can also extrapolate to the critical momentum, assuming, that the prediction of renormalization group equations^{6,7} is correct:

$$\Delta_3(p, \gamma = 0) = S_3(p, \gamma = 0) + \ln \left(1 - \frac{p}{\pi}\right) = B \cdot \left[-\ln \left(1 - \frac{p}{\pi}\right)\right]^{3/2} \quad \text{for } p \rightarrow \pi. \quad (3.10)$$

In this case we obtain for coefficient B :

$$B \simeq 0.05. \quad (3.11)$$

Of course the vicinity of the minimum at $p = p(\gamma) = 0.82\pi$, prevents us to decide, whether (3.8) or (3.10) is the correct form at the critical momentum $p = \pi$.

IV. FINITE SIZE ANALYSIS OF THE STRUCTURE FACTORS AT THE CRITICAL MOMENTUM

The finite size ansatz (3.1) breaks down for the “critical” momentum $p = \pi$. The exponent of N^{-1} changes from a fixed to an η_j dependent value:

$$S_j(p = \pi, \gamma, N) = r_j(\gamma) \cdot \frac{\eta_j}{\eta_j - 1} \left[1 - \left(\frac{N}{N_j(\gamma)}\right)^{1-\eta_j} + \dots \right]. \quad (4.1)$$

We have plotted in Fig. 9 the longitudinal and transverse structure factors at the critical momentum $p = \pi$ versus:

$$\frac{\eta_j}{\eta_j - 1} \left[1 - \sin \left(\frac{\pi}{2}\eta_j\right) \cdot N^{1-\eta_j} \right], \quad j = 1, 3. \quad (4.2)$$

We observe an almost linear behavior in this variable. A tiny nonlinearity appears in the longitudinal structure factor if we approach the isotropic limit $\gamma \rightarrow 0$, where (4.2) reduces to $\ln N$. The variable (4.2) enables us to compare the longitudinal and transverse structure factors at momentum $p = \pi$. In particular, we can see how the two structure factors converge to each other in the isotropic limit. In this limit the coefficient in front of the right hand side of (4.1) develops a pole, such that we find for the structure factors:

$$S_j(p = \pi, \gamma = 0, N) \xrightarrow{N \rightarrow \infty} r_j(0) \ln \left(\frac{N}{N_j(0)}\right). \quad (4.3)$$

For a precise determination of $r_1(0), r_3(0), N_1(0), N_3(0)$ we have repeated the computation of the structure factors for small γ values ($\gamma/\pi = 0.01, 0.02, 0.03, 0.04, 0.05$). The fit to the ansatz (4.1) yields for the parameters $r_j(\gamma)$ and $N_j(\gamma)$ as function of $L_j(\pi, \gamma)^{-1} = (\eta_j - 1)/\eta_j$, the curves shown in Fig. 10.

The parameters $r_3(\gamma), r_1(\gamma)$ and $N_3(\gamma), N_1(\gamma)$ determined in this way converge to each other. Of course, we should have in mind, that our finite size analysis (4.1) takes into account only the first two terms of an infinite expansion. Approaching the isotropic limit, it might happen that subleading terms compete more and more with the leading ones. Such an effect could spoil our determination of $r_1(0), r_3(0), N_1(0), N_3(0)$.

In Fig. 9 the small deviations from linearity for $\gamma = 0.1\pi$ might originate from subleading terms. The summation of these terms might also change the exponent of $\ln N$ in the isotropic structure factor (4.3). This exponent is predicted to be 3/2 instead of 1 by renormalization group equations.^{6,7} We think, however, that it is impossible to extract this exponent in a reliable way from the small systems we are investigating here.

V. FINITE SIZE SCALING VARIABLES FOR ALL MOMENTUM VALUES.

The finite size effects (3.1) for $p < \pi$ and (4.1) for $p = \pi$ can be properly described by the scaling ansatz

$$S_j(p, \gamma, N) = S_j(\gamma, L_j(p, \gamma, N)), \quad j = 1, 3, \quad (5.1)$$

with a size dependent modification of the scaling variables (2.1) and (2.5):

$$L_j(p, \gamma, N) = \frac{\eta_j}{2(\eta_j - 1)} \left[\left(1 + i \frac{a_j}{N}\right)^{\eta_j - 1} + \left(1 - i \frac{a_j}{N}\right)^{\eta_j - 1} - \left(1 - \frac{p}{\pi} + i \frac{a_j}{N}\right)^{\eta_j - 1} - \left(1 - \frac{p}{\pi} - i \frac{a_j}{N}\right)^{\eta_j - 1} \right]. \quad (5.2)$$

The $L_j(p, \gamma, N)$ have the following properties:

(1) There is no finite size effect for:

$$L_3(p, \gamma = \pi/2, N) = \frac{2}{\pi} p. \quad (5.3)$$

(2) For $p \neq \pi, \gamma \neq 0$ the leading finite size effects are of the form:

$$L_j(p, \gamma, N) - L_j(p, \gamma) = \frac{\eta_j(2 - \eta_j)}{2} \left[1 - \left(1 - \frac{p}{\pi}\right)^{\eta_j - 3} \right] \cdot \left(\frac{a_j}{N}\right)^2. \quad (5.4)$$

(3) For $p = \pi$ and $\gamma \neq 0$ the leading finite size behavior changes to:

$$L_j(p = \pi, \gamma, N) = \frac{\eta_j}{\eta_j - 1} \left[1 - \sin\left(\frac{\pi}{2}\eta_j\right) \left(\frac{a_j}{N}\right)^{\eta_j - 1} \right]. \quad (5.5)$$

(4) For the isotropic case $\gamma = 0$ (5.2) reduces to:

$$L_j(p, \gamma = 0, N) = \frac{1}{2} \ln \frac{1 + (a_j/N)^2}{(1 - p/\pi)^2 + (a_j/N)^2}. \quad (5.6)$$

The quantities a_j in (5.2) can still depend on p and γ . For $p < \pi, \gamma > 0$, they are related to the coefficients $c_j(p, \gamma)$ describing the finite size behavior (3.1):

$$c_j(p, \gamma) = \frac{\partial S_j}{\partial L_j} \cdot \frac{\eta_j(2 - \eta_j)}{2} \cdot \left[1 - \left(1 - \frac{p}{\pi}\right)^{\eta_j - 3} \right] a_j(p, \gamma)^2. \quad (5.7)$$

The derivative of the scaling functions $S_j(\gamma, L_j)$ with respect to the scaling variable L_j is close to one up to the small deviations coming from the difference $\Delta_j(p, \gamma)$ depicted in Figs. 7(a)-(f). Note that the size dependent scaling variable (5.2) describes correctly the singularity structure (3.2) of $c_j(p, \gamma)$ for $p \rightarrow \pi, \gamma > 0$. Therefore the quantities $a_j(p, \gamma)$ are expected to be free of singularities for $p = \pi$.

Under the premise that the scaling ansatz (5.1) is correct and the finite size behavior at $p = \pi$ is given by (4.1), the scaling function in (5.1) has to increase linearly with the scaling variable (5.2) for large values of L_j . In particular, we find for the diverging transverse structure factor at $p = \pi$ and $N \rightarrow \infty$:

$$S_1(\gamma, L_1(p, \gamma, N)) \Big|_{p=\pi} \xrightarrow{N \rightarrow \infty} r_1(\gamma) \cdot \frac{\eta_1}{\eta_1 - 1} \left[1 - \sin\left(\frac{\pi}{2}\eta_1\right) \left(\frac{a_1}{N}\right)^{\eta_1 - 1} \right]. \quad (5.8)$$

Comparing with (4.1) we see that the scaling ansatz (5.1) with the scaling variable (5.2) provides us as well with the singular behavior of the coefficient on the right hand side of (4.1) in the isotropic limit $\gamma \rightarrow 0$. Moreover there is a relation between $N_1(\gamma)$ and $a_1(p = \pi, \gamma)$:

$$N_1(\gamma) = a_1(p = \pi, \gamma) \cdot \left(\sin \frac{\pi}{2}\eta_1\right)^{-\pi/\gamma}. \quad (5.9)$$

In contrast to the transverse structure factor, the longitudinal one stays finite for $p = \pi, N \rightarrow \infty, \gamma > 0$. The comparison of (4.1) with the scaling ansatz (5.1) and (5.2) yields here:

$$S_3(\gamma, L_3(p, \gamma))|_{p=\pi} = r_3(\gamma) \frac{\eta_3}{\eta_3 - 1}, \quad (5.10)$$

$$N_3(\gamma) = a_3(p = \pi, \gamma) \cdot \left[\frac{\partial \ln S_3}{\partial L_3} \cdot \frac{\eta_3}{\eta_3 - 1} \sin\left(\frac{\pi}{2}\eta_3\right) \right]^{\pi/\gamma-1}. \quad (5.11)$$

Again we find the pole in the coefficient on the right hand side of (4.1), provided that the scaling function $S_3(\gamma, L_3)$ increases linearly with $L_3(p = \pi, \gamma)$ [cf.(2.3)]. The linear behavior also guarantees that $N_1(\gamma)$ [cf.(5.9)] and $N_3(\gamma)$ [cf.(5.11)] converge to the same value if:

$$a_1(p = \pi, \gamma = 0) = a_3(p = \pi, \gamma = 0). \quad (5.12)$$

Summarizing we can say: The scaling ansatz (5.1) with the scaling variable (5.2) reproduces correctly:

- (1) The finite size behavior (3.1) at $p < \pi$ and (4.1) at $p = \pi$.
- (2) The singular behavior (3.2) of the coefficients $c_j(p, \gamma)$ for $p \rightarrow \pi$.
- (3) The singular behavior of the coefficients on the right hand side of (4.1) for $\gamma \rightarrow 0$.

On the other hand, the quantities $a_j(p, \gamma)$, which enter in the definition of the scaling variable (5.2) appear to be free of singularities at $p = \pi$ and $\gamma = 0$.

Finally, we would like to mention that the term $a_j N^{-1}$ in (5.2) can be interpreted as an inverse correlation length $\xi_j(\gamma, N)^{-1}$. The Fourier transform of (5.2) which brings us back to the configuration space (with coordinate x) has a large distance behavior:

$$\frac{(-1)^x}{x^{\eta_j}} \exp\left(-\frac{x}{\xi_j(\gamma, N)}\right). \quad (5.13)$$

The effective correlation length $\xi_j(\gamma, N) = N/a_j$ takes into account the finiteness of the system. In the critical regime $0 \leq \gamma \leq \pi/2$ —we are considering here— the effective correlation length is assumed to increase with the system size N .

VI. CONCLUSION

In this paper we have analysed the longitudinal and transverse structure factors $S_j(p, \gamma, N)$ of the XXZ model on finite rings $N \leq 28$. Based on this analysis we got a reliable estimate of the thermodynamical limits $N \rightarrow \infty$ for momenta $p \leq 13\pi/14$ and for $\gamma/\pi = 0, 0.1, 0.2, 0.3, 0.4, 0.5$. We observe two kinds of structures:

- (1) A “gross”-structure, which is given by the universal scaling variables (2.1) and (2.5).
- (2) A “fine”- structure, which contributes only a few percents and which depends explicitly on γ . In particular we found a minimum in the longitudinal structure factors at momentum $p = p(\gamma)$ listed in TABLE I. A comparison of our finite size analysis with the exact result⁹ on the structure factors in the XX model ($\gamma = \pi/2$) yields excellent agreement.

A comparison with the conjecture of Müller¹⁰ *et al.* reveals systematic deviations for the transverse structure factors and striking discrepancies for the longitudinal structure factors.

Exact diagonalizations of the Hamiltonian – as they were performed in this paper for the XXZ-model – are restricted to rather small systems ($N \lesssim 36$) in contrast to quantum Monte Carlo simulations which are feasible on much larger systems ($N \lesssim 1000$). Monte Carlo simulations, however, suffer under statistical errors, which simply prevent the resolution of the “fine”-structures mentioned above.

On the other hand these structures are clearly visible in exact calculations on small systems and we are sure that they survive in the thermodynamical limit for the following reason. The finite size effects of the structure factors $S_j(p, \gamma, N)$, $j = 1, 3$ are well under control, which we demonstrated by comparison with the exact result for the XX case ($\gamma = \pi/2$). It should be possible to extend this type of finite size analysis to the dynamical structure factors. Work along this line is in progress.

APPENDIX A:

We are going to prove that the longitudinal structure factors for the groundstate on a ring with N sites is given by:

$$S_3(p = 2\pi k/N, \gamma = \pi/2, N) = \frac{4k}{N}, \quad k = 0, 1, \dots, \frac{N}{2}, \quad (\text{A1})$$

which means for spin-spin correlators in the groundstate $|0\rangle$:

$$4\langle 0|S_3(0)S_3(x)|0\rangle(\gamma = \pi/2, N) = \begin{cases} 1 & \text{for } x = 0 \\ 0 & \text{for } x = 2l \\ -\frac{4}{N^2 \sin^2(\pi x/N)} & \text{for } x = 2l + 1. \end{cases} \quad (\text{A2})$$

Following Lieb, Schultz and Mattis⁸ the spin-spin correlators can be represented as:

$$4\langle 0|S_3(0)S_3(l)|0\rangle(\gamma = \pi/2, N) = (G_0^\sigma)^2 - (G_l^\sigma)^2, \quad (\text{A3})$$

where

$$G_l^\sigma = - \sum_{k=0}^{N-1} \Phi_{k0}^\sigma \Phi_{kl}^\sigma \text{sgn}(\Lambda_k^\sigma). \quad (\text{A4})$$

The Φ_{kl}^σ are solutions of the equations:

$$\Phi_{k2}^\sigma + \sigma \Phi_{kN}^\sigma = \Lambda_k^\sigma \Phi_{k1}^\sigma, \quad (\text{A5a})$$

$$\Phi_{k,l-1}^\sigma + \Phi_{k,l+1}^\sigma = \Lambda_k^\sigma \Phi_{kl}^\sigma, \quad (\text{A5b})$$

$$\sigma \Phi_{k1}^\sigma + \Phi_{k,N-1}^\sigma = \Lambda_k^\sigma \Phi_{kN}^\sigma. \quad (\text{A5c})$$

These equations are obtained by the diagonalization of the XX Hamiltonian by means of a Jordan-Wigner-Transformation. In the derivation of these equations one has to distinguish between the chains $N = 4, 8, 10, \dots$; ($\sigma = -1$) and $N = 6, 10, 14, \dots$; ($\sigma = +1$). Indeed equations (A5) were derived by Lieb, Schultz and Mattis⁸ for $\sigma = 1$. The derivation for the second case is straight forward. It is easy to verify that the equations (A5) are solved by:

$$\Phi_{kl}^+ = \sqrt{\frac{2}{N}} \begin{cases} 1/\sqrt{2} & \text{for } k = 0 \\ \cos(2kl\pi/N) & \text{for } k = -1, -2, \dots, -N/2 + 1 \\ \sin(2kl\pi/N) & \text{for } k = +1, 2, \dots, N/2 - 1 \\ (-1)^l/\sqrt{2} & \text{for } k = N/2, \end{cases} \quad (\text{A6a})$$

$$\Phi_{kl}^- = \sqrt{\frac{2}{N}} \begin{cases} \cos[(2k+1)l\pi/N] & \text{for } k = 0, -1, \dots, -N/2 + 1 \\ \sin[(2k+1)l\pi/N] & \text{for } k = +1, 2, \dots, N/2, \end{cases} \quad (\text{A6b})$$

$$\Lambda_k^\sigma = \cos \left[\frac{\pi}{N} \left(2k + \frac{1}{2}(1 - \sigma) \right) \right], \quad k = -\frac{N}{2} + 1, -\frac{N}{2}, \dots, \frac{N}{2}. \quad (\text{A6c})$$

Our proof of (A1) is completed if we insert these solutions into (A4) and (A3).

* e-mail: muetter@wpts0.physik.uni-wuppertal.de

¹ M. Karbach and K.H. Mütter, Z. Phys. B**90**, 83 (1993).

² A. Luther and I. Peschel, Phys. Rev. B**12**, 3908 (1975); H.C. Fogedby, J. Phys. C**11**, 4767 (1978).

³ V.E. Korepin and A.G. Izergin, Commun. Math. Phys. **94**, 67 (1984); **99**, 271, (1985); Pis'ma. Zh. Eksp. Teor. Fiz. **42**, 414 (1985) [Sov. Phys. -JETP Lett. **42**, 512 (1985)]; N.M. Bogoliubov, A.G. Izergin, and V.E. Korepin, Nucl. Phys. B**275**, 687 (1986).

⁴ N.M. Bogoliubov, A.G. Izergin, and N.Y. Reshetikhin, Pis'ma. Zh. Eksp. Teor. Fiz. **44**, 405 (1986) [Sov. Phys. -JETP Lett. **44**, 521 (1986)]; J. Phys. A**20**, 5361 (1987).

⁵ J.D. Johnson, S. Krinsky, and B.M. McCoy, Phys. Rev. A**8**, 2526 (1973).

⁶ R.R.P. Singh, M.E. Fisher, and R. Shankar, Phys. Rev. B**39**, 2562 (1989).

⁷ I. Affleck, D. Gepner, H.J. Schulz, and T. Ziman, J. Phys. A**22**, 511 (1989); K. Nomura, Phys. Rev. B**48**, 16814 (1993).

⁸ E. Lieb, T. Schultz, and D. Mattis, Ann. Phys. **16**, 407 (1961).

⁹ T. Tonegawa, Solid State Commun. **40**, 983 (1981).

¹⁰ G. Müller, H. Thomas, H. Beck, and J.C. Bonner, Phys. Rev. B**24**, 1429 (1981); G. Müller, H. Thomas, M.W. Puga and, H. Beck, J. Phys. C**14** 3399, (1981).

FIGURE CAPTIONS

FIG. 1. The longitudinal structure factor versus the scaling variable (2.1) for $\gamma/\pi = 0, 0.1, 0.2, 0.3, 0.4, 0.5$ and $N = 4, 6, \dots, 28$.

FIG. 2. The difference (2.3) versus the scaling variable (2.1).

FIG. 3. Same as Fig. 1 for the transverse structure factor versus the scaling variable (2.5).

FIG. 4. The difference (2.6) versus the scaling variable (2.5).

FIG. 5. Finite size analysis of $\Delta_j(p, \gamma, N)$ at momentum $p = \pi/2$:

- (a) for the longitudinal structure factor,
- (b) for the transverse structure factor.

FIG. 6. The coefficient $c_j(p, \gamma)$, $j = 1, 3$ in the finite size ansatz (3.1) as a function of (3.2).

FIG. 7. The thermodynamical limit $N \rightarrow \infty$ of the transverse structure factor:

- T1: our finite size analysis
- T2: conjecture Ref. 10
- T3: exact result Ref. 9 at $\gamma = \pi/2$

and of the longitudinal structure factor:

- L1: our finite size analysis
- L2: conjecture Ref. 10

(a) $\gamma = 0.5\pi$, (b) $\gamma = 0.4\pi$, (c) $\gamma = 0.3\pi$, (d) $\gamma = 0.2\pi$, (e) $\gamma = 0.1\pi$, (f) $\gamma = 0$.

FIG. 8. The scaling function $g_j(z = 2, \gamma)$, $j = 1, 3$ in the finite size scaling ansatz (3.4) as a function of γ .

FIG. 9. Large N behavior of the structure factors (4.1) at the critical momentum $p = \pi$.

FIG. 10. The coefficients $r_j(\gamma), N_j(\gamma)$ $j = 1, 3$ in the finite size ansatz (4.1) as a function of $L_j(p, \gamma)^{-1}$,
 (a) $r_j(\gamma)$, (b) $N_j(\gamma)$.

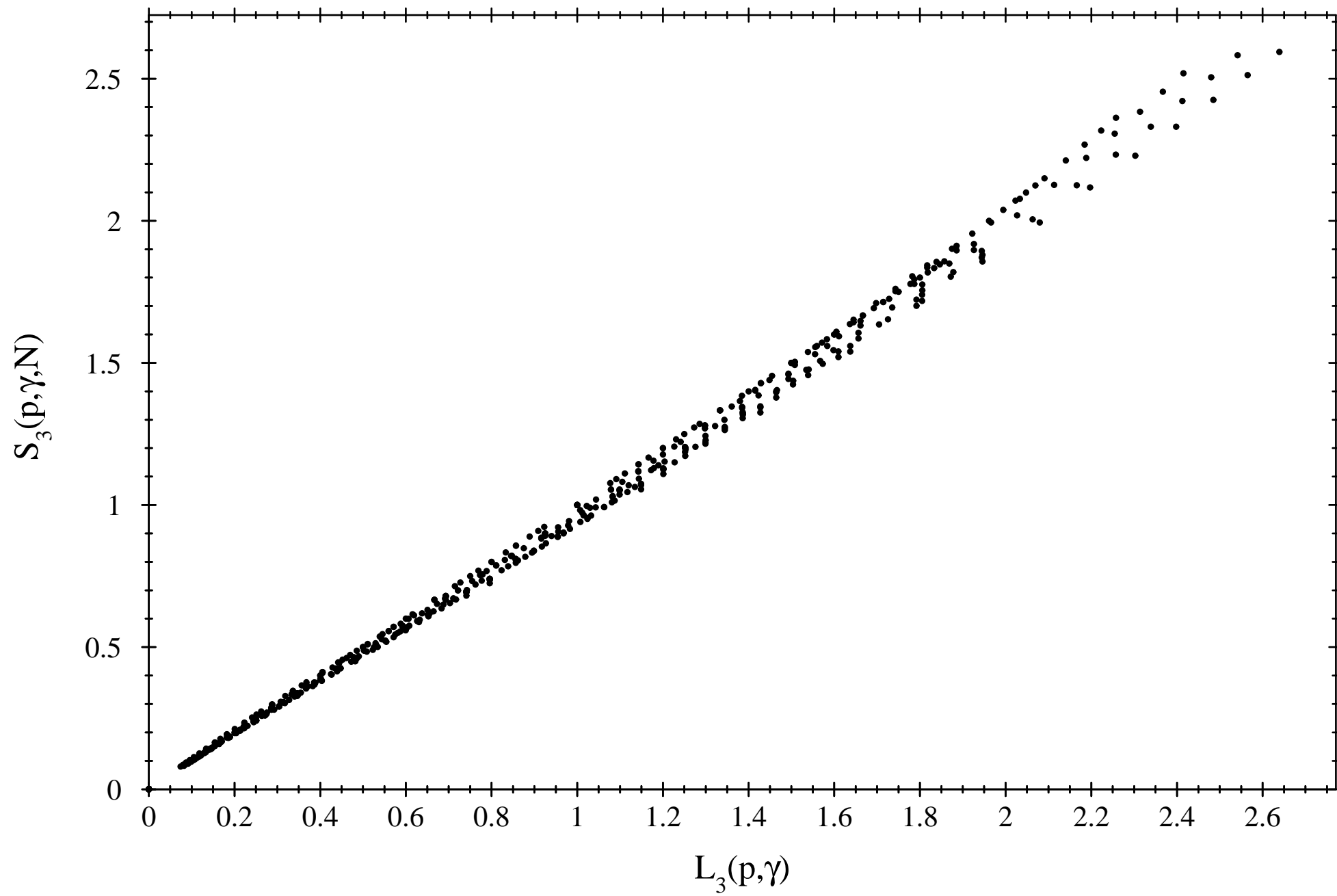


FIG.
karba

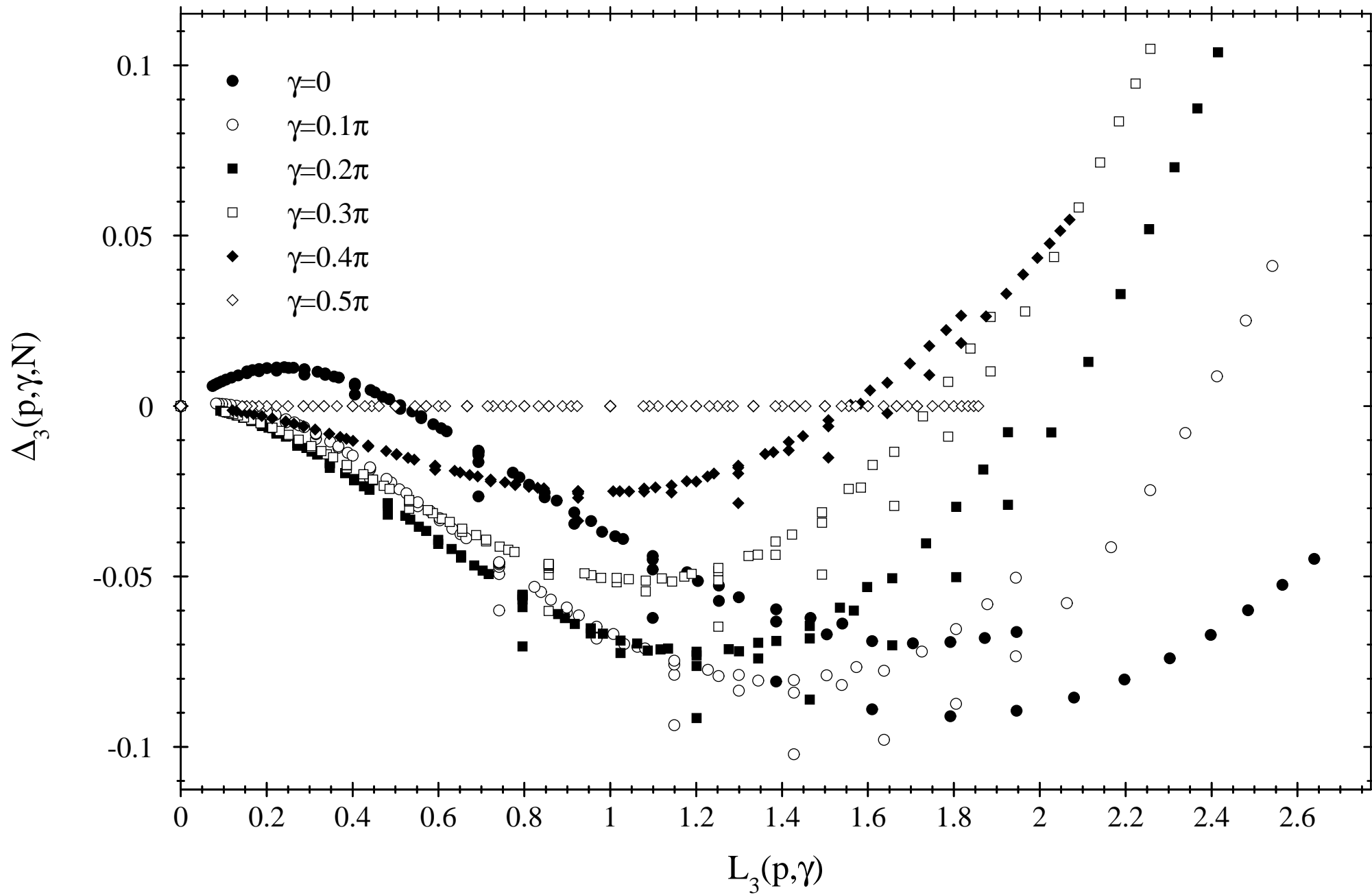


FIG. 1
karba

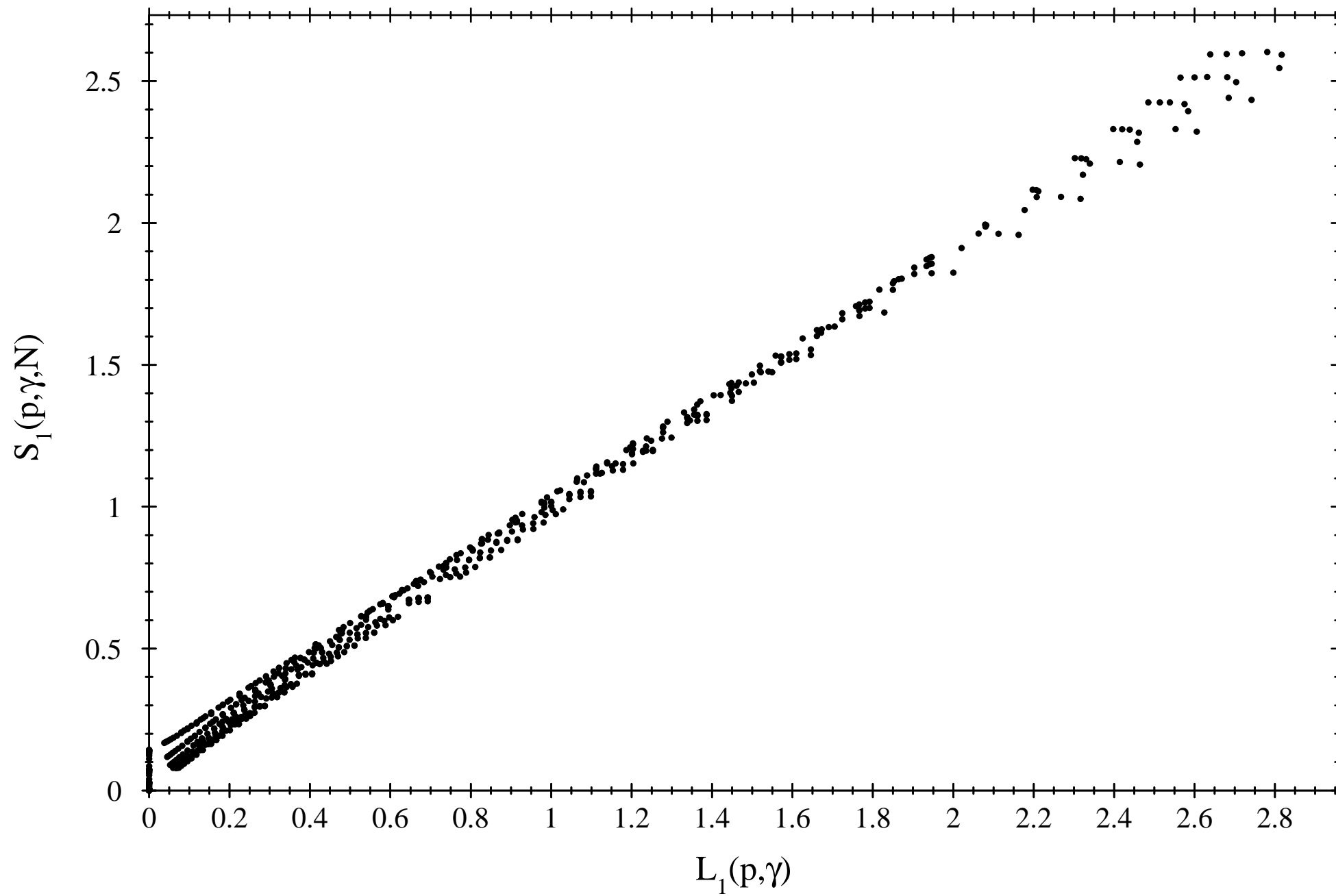


FIG.
karba

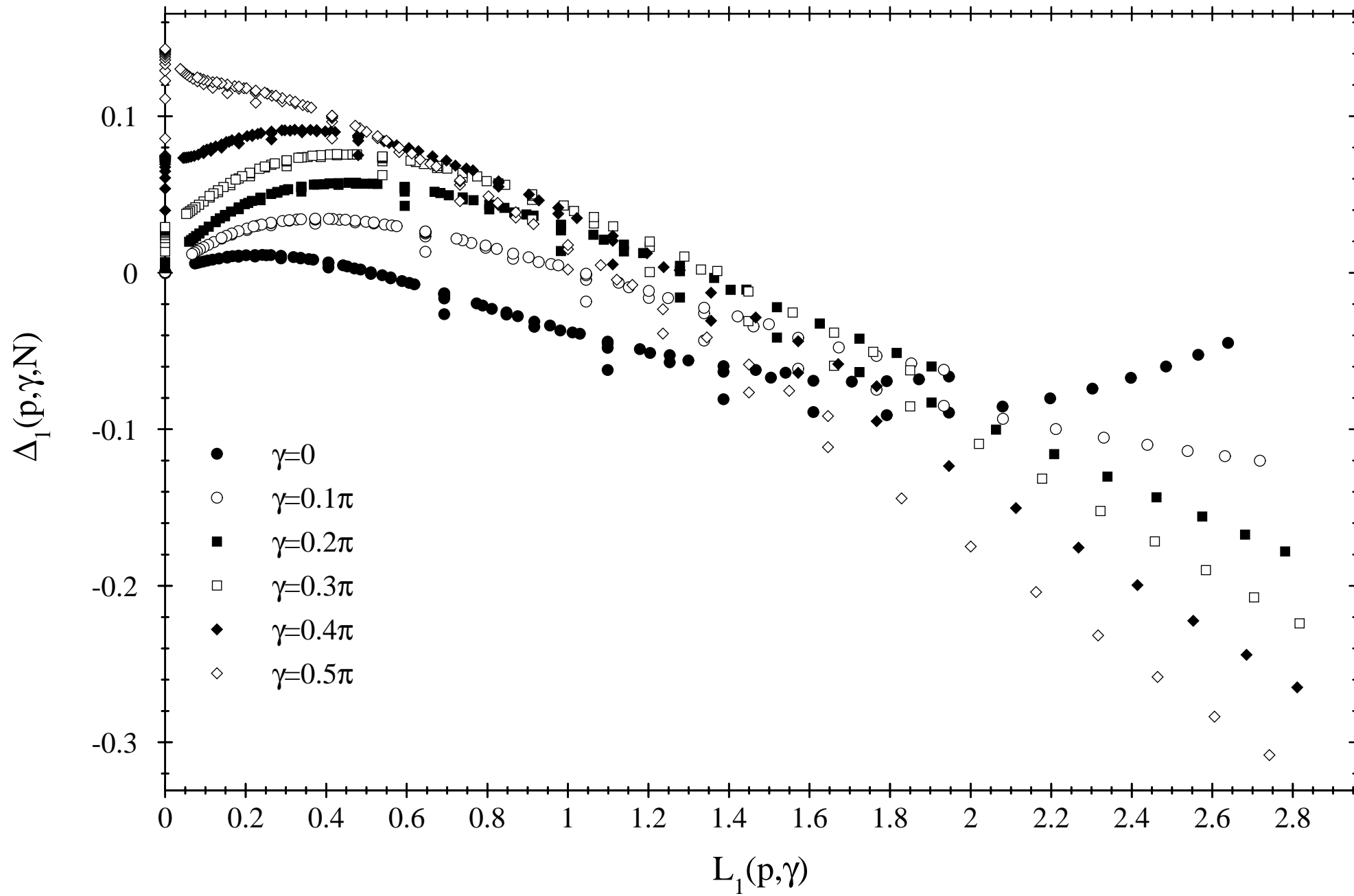


FIG. .
karba

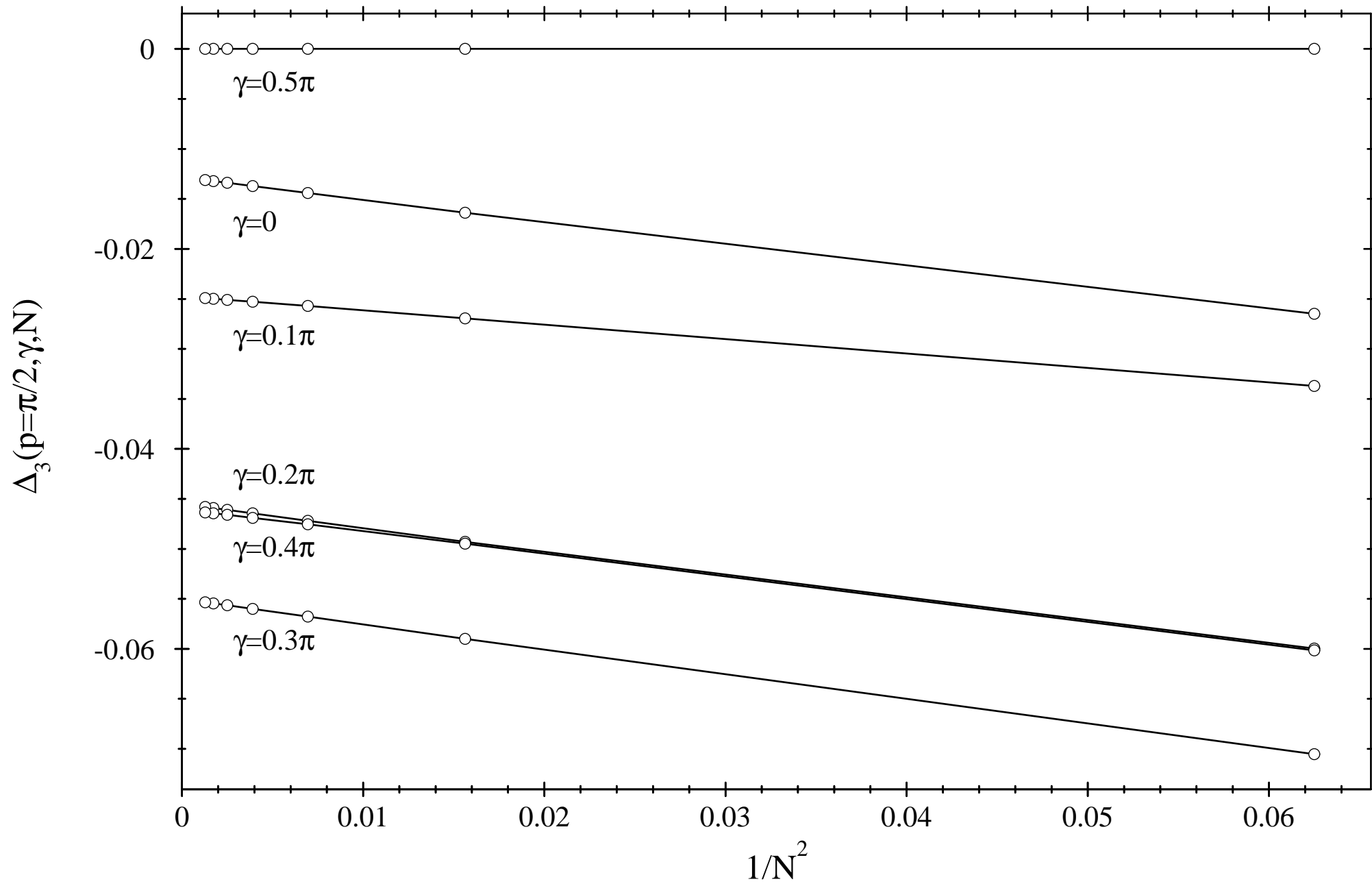


FIG.
karba

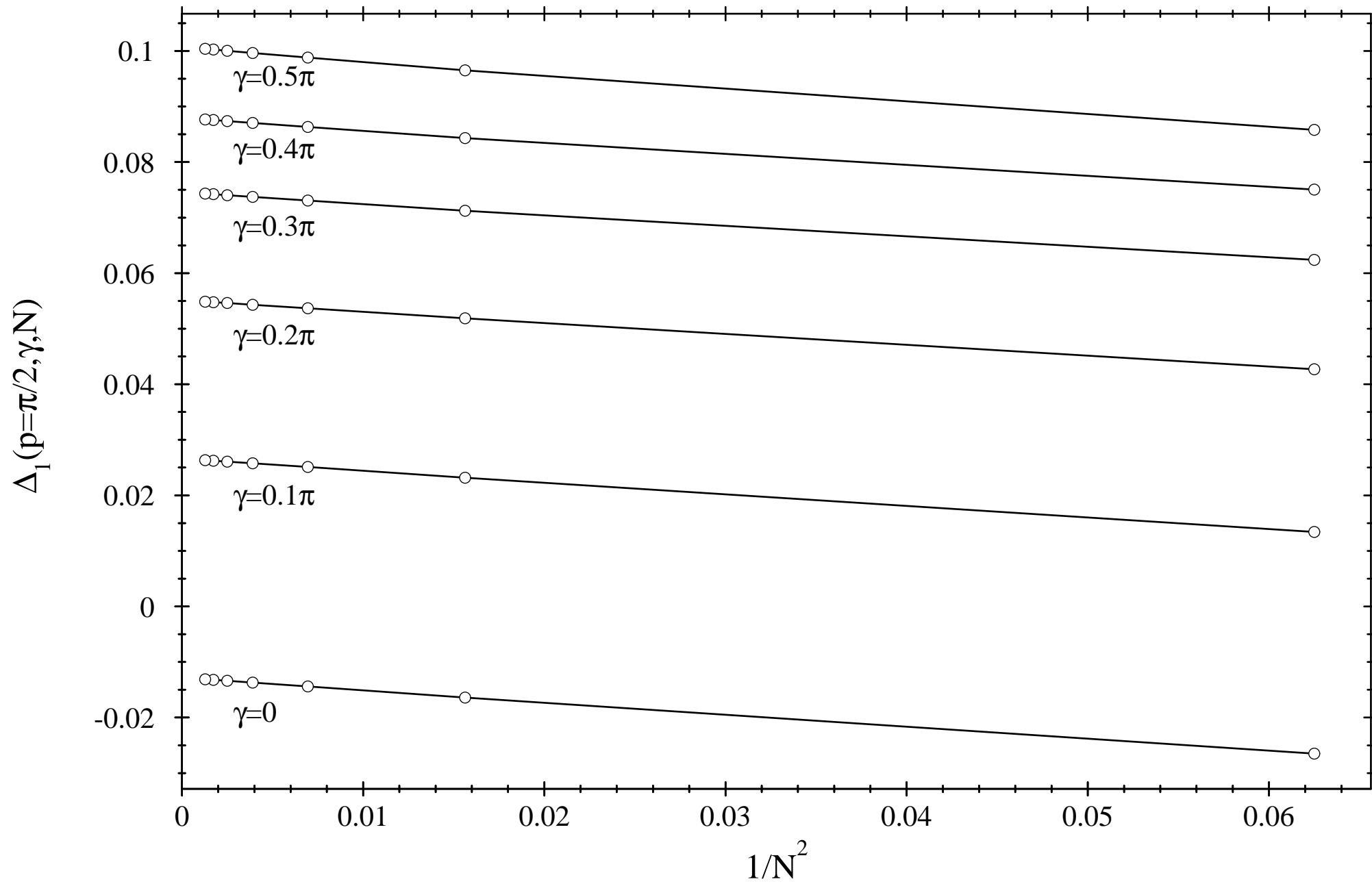


FIG.
karba

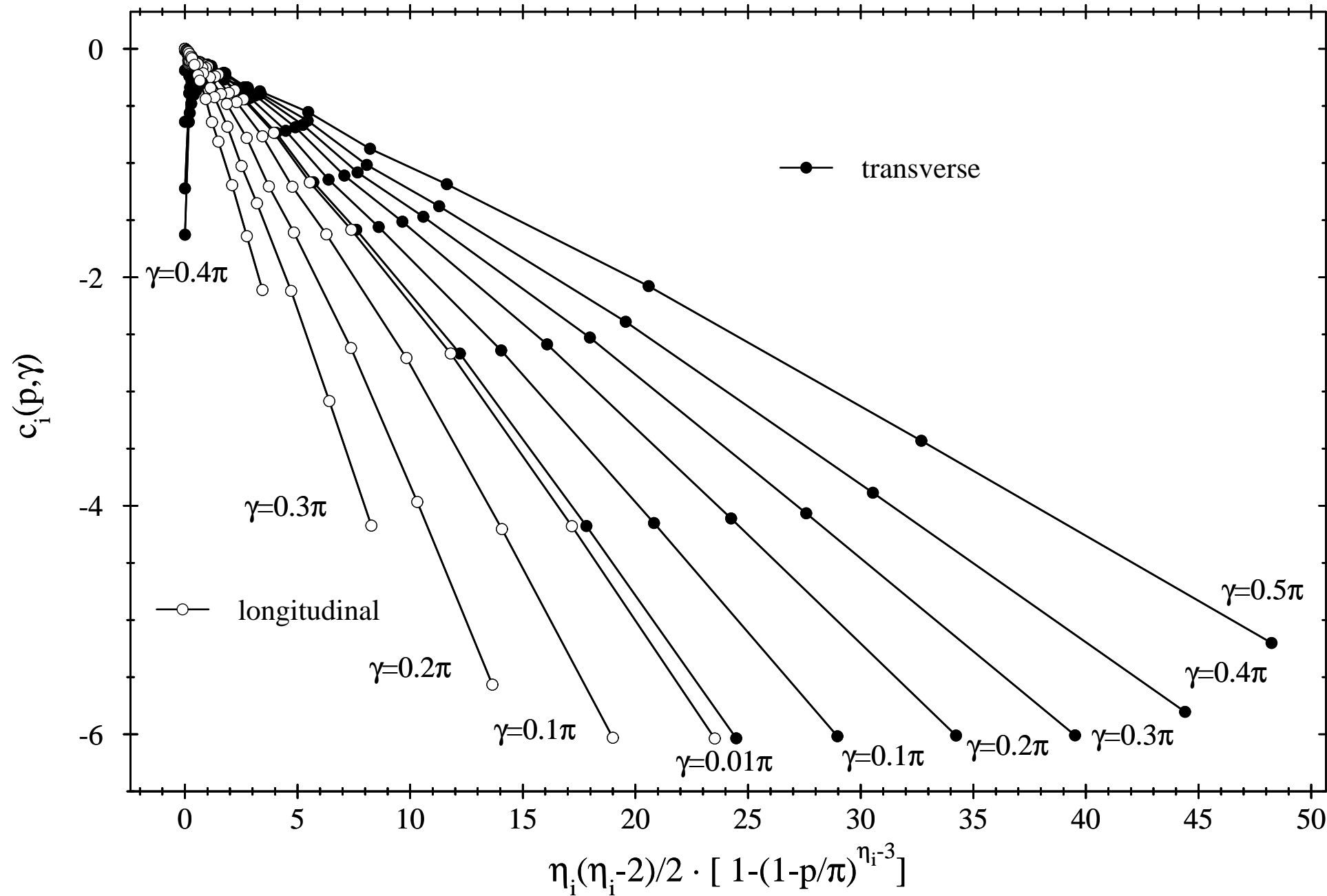


FIG.
 karba

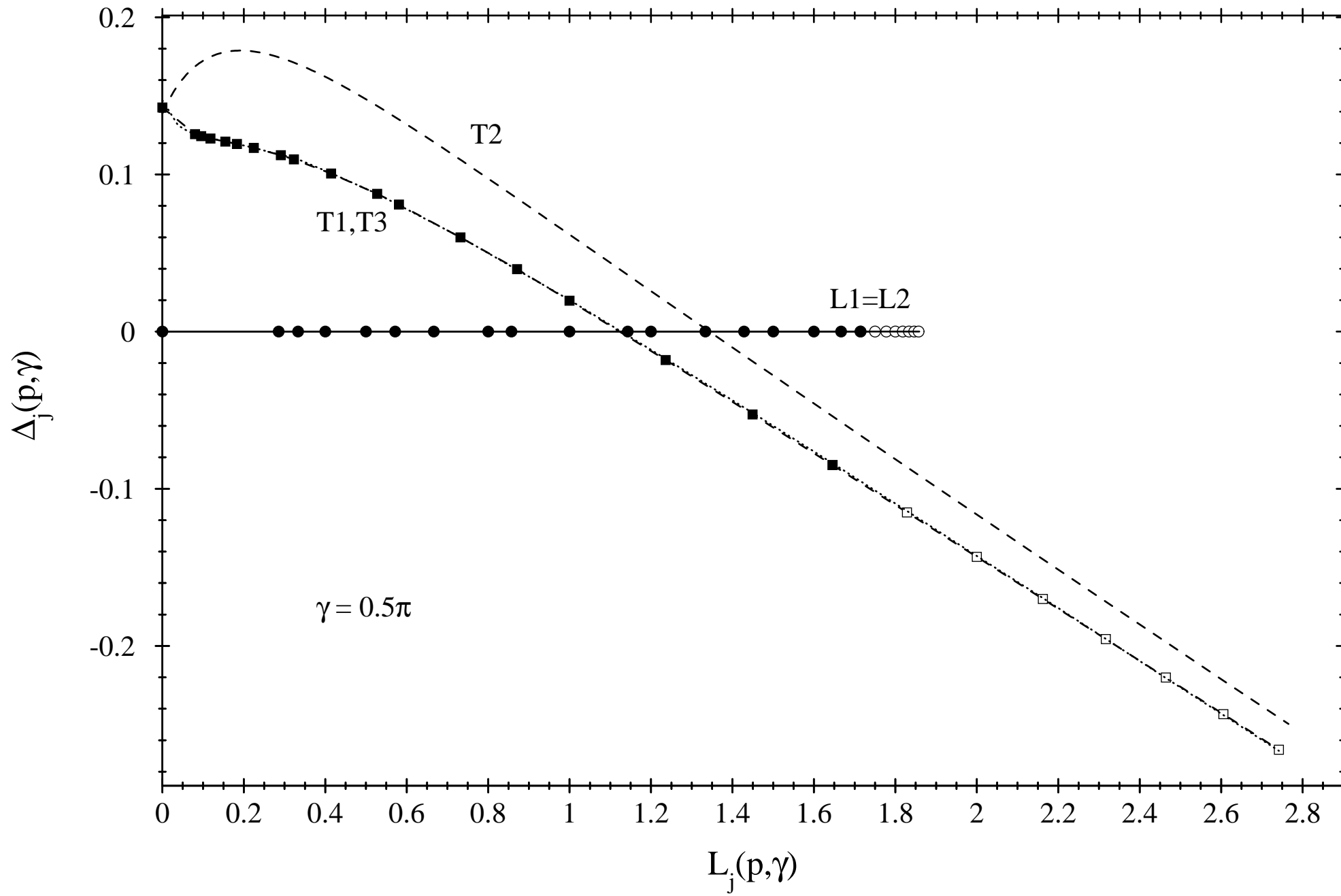


FIG. 1
karba

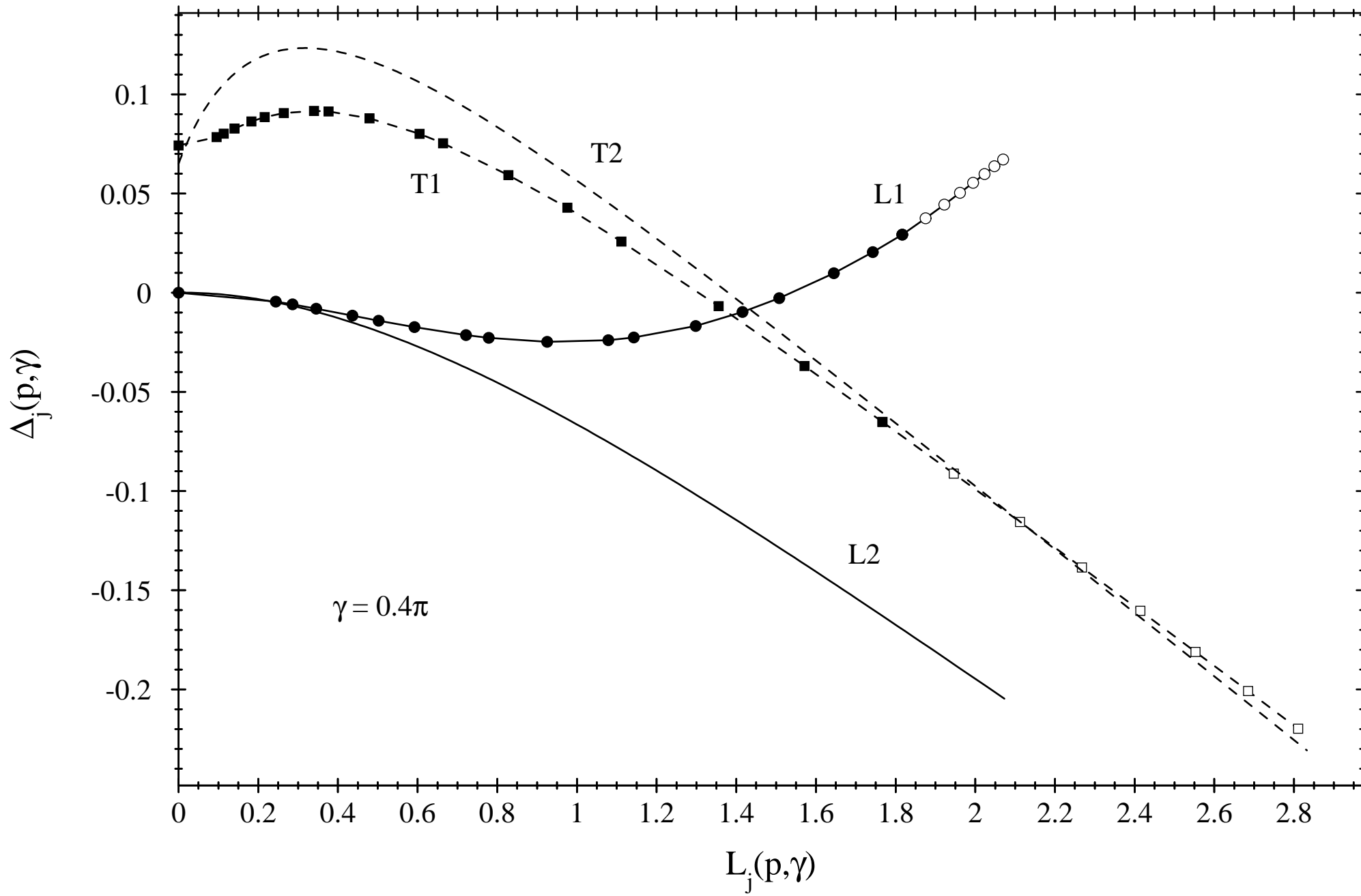


FIG. 1
 karba...

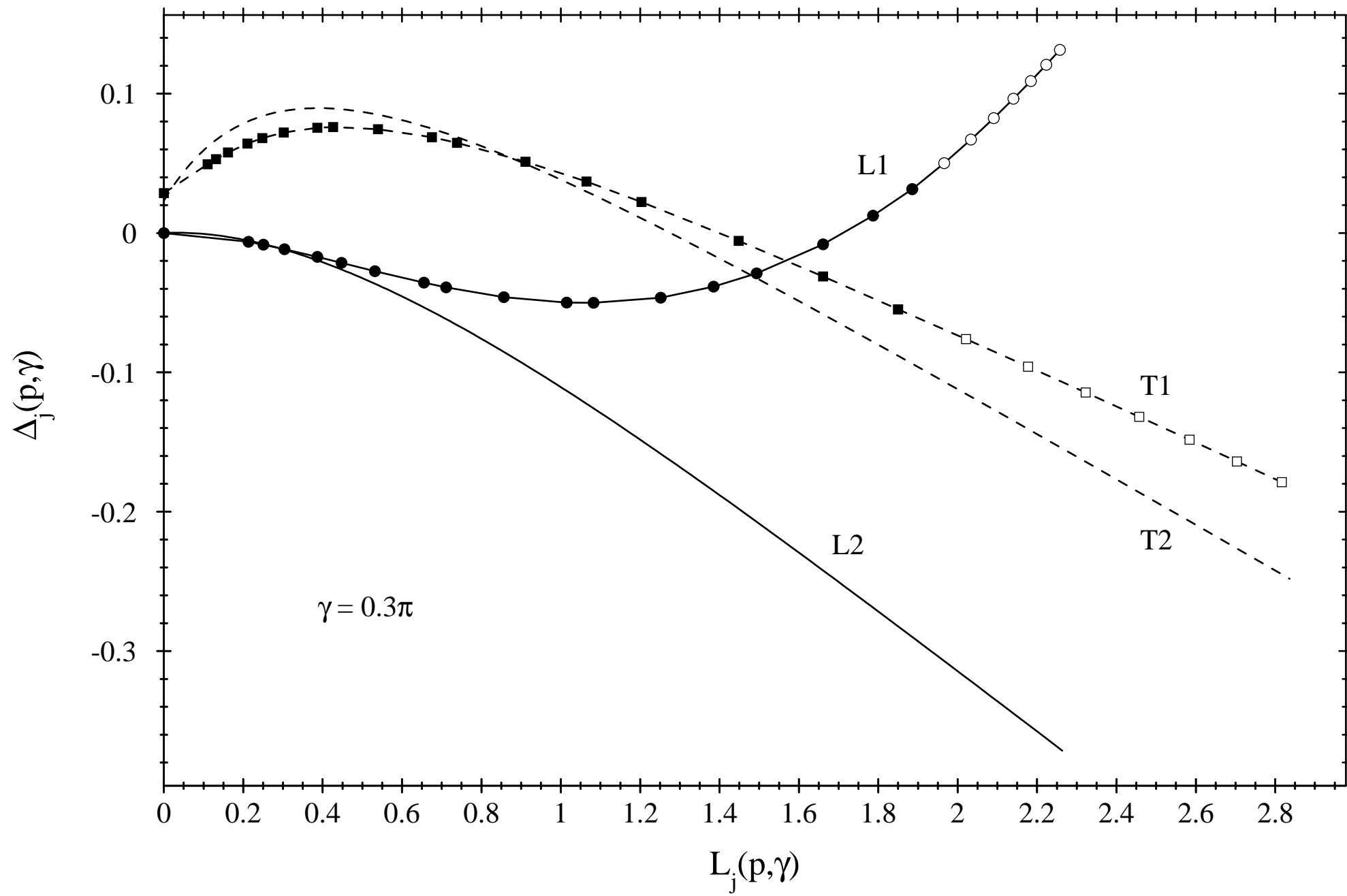


FIG. 1
 karba...

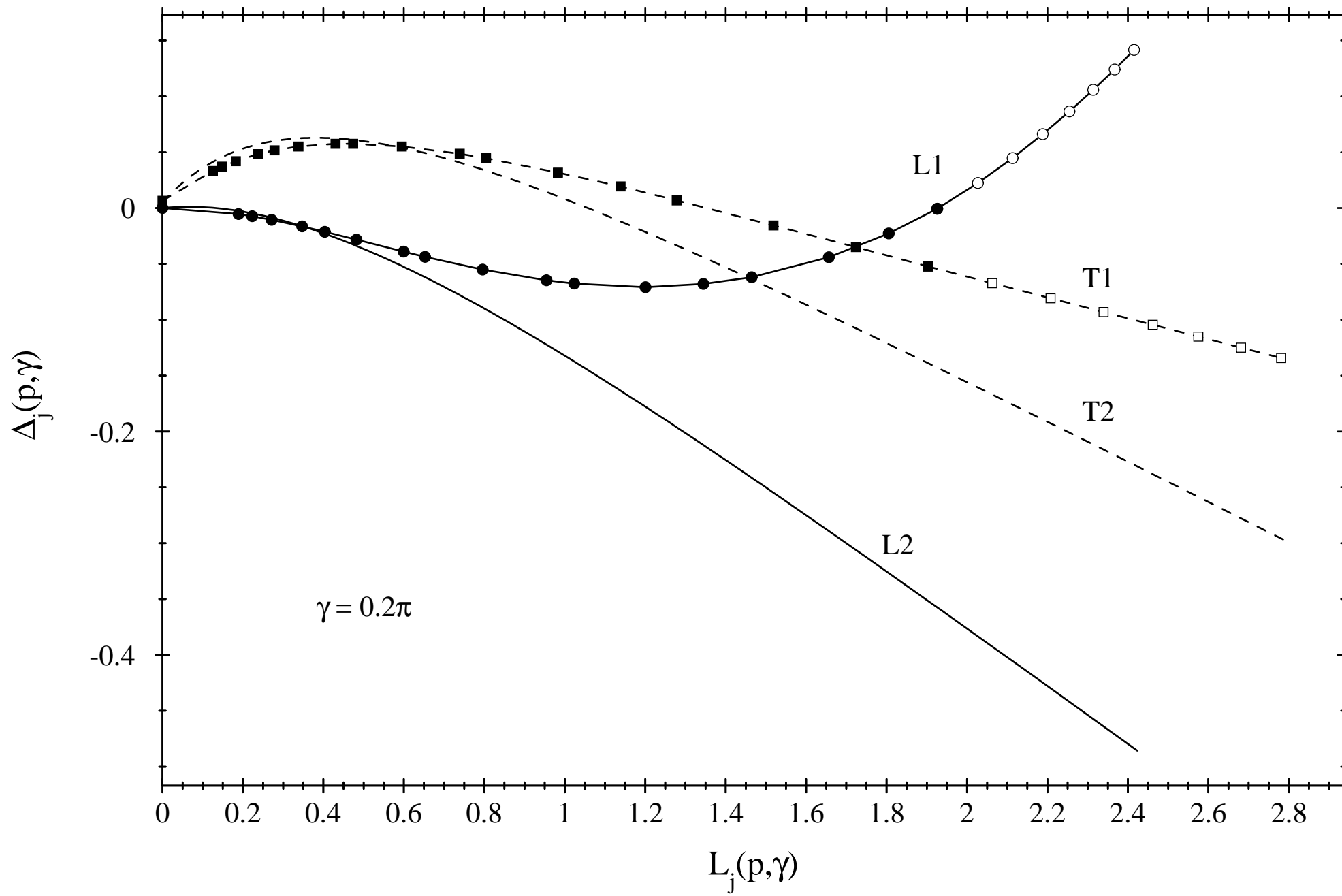


FIG. 1
 karba

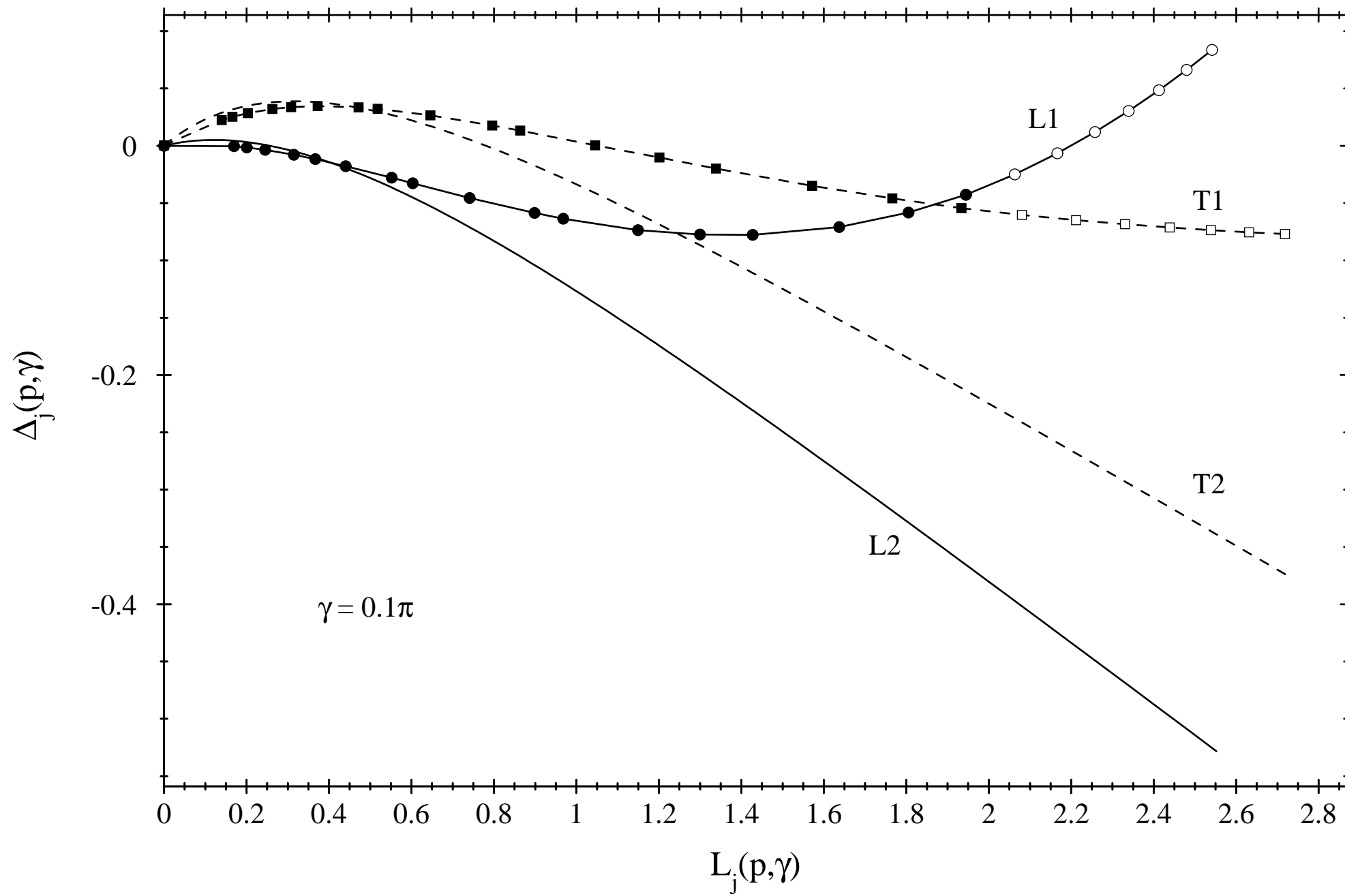


FIG. 1
karba

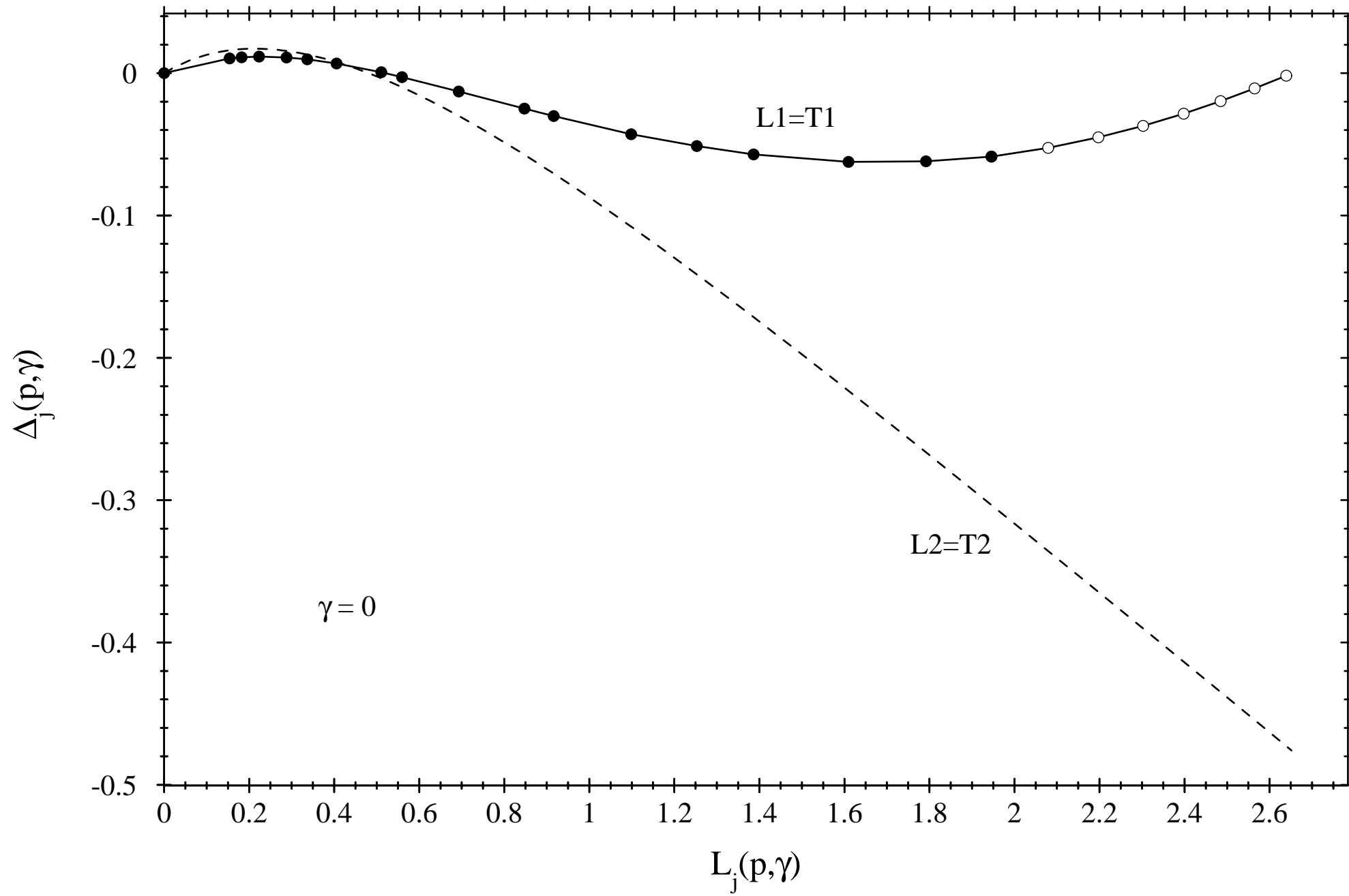


FIG. 1
 karba

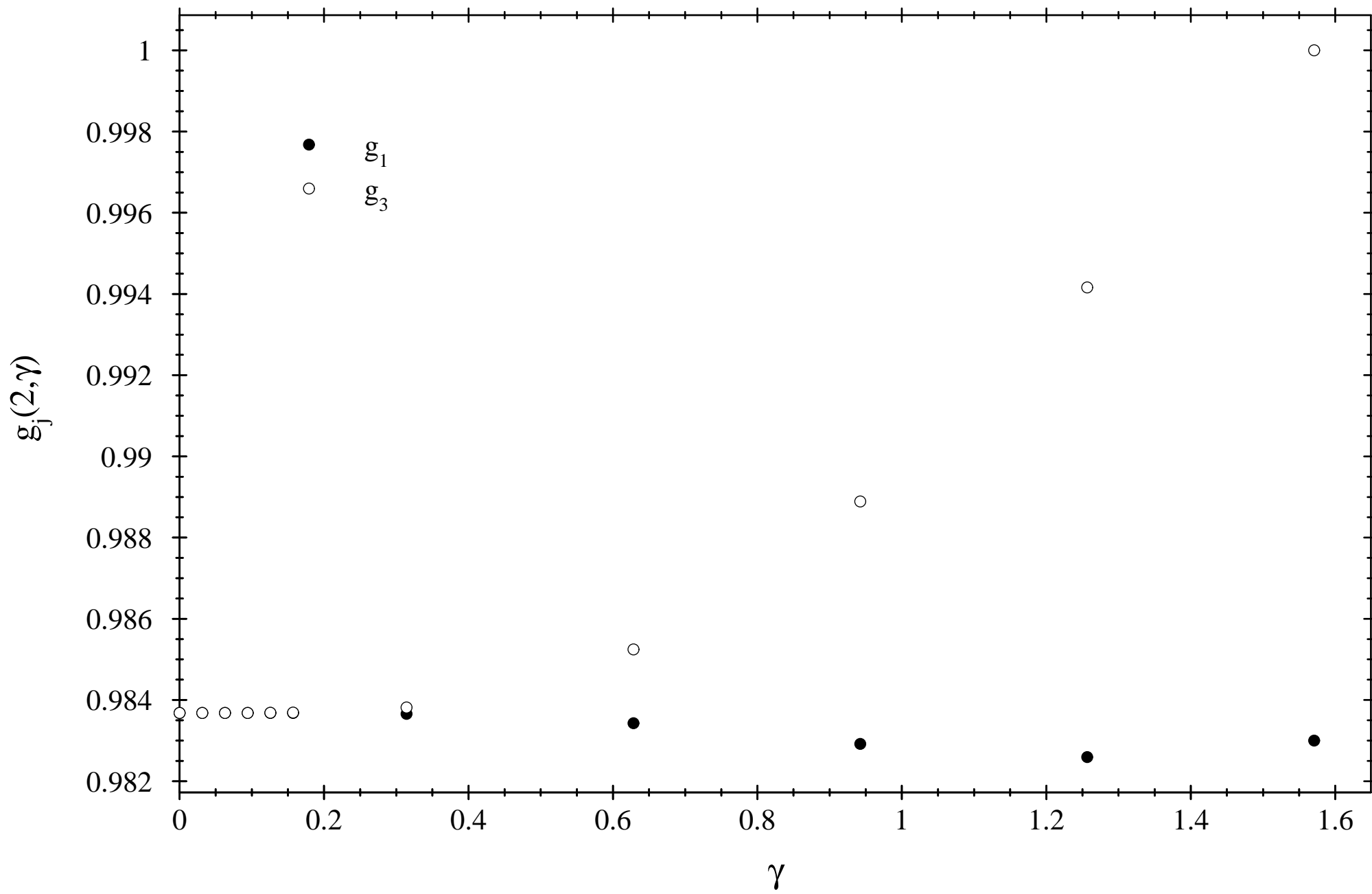


FIG.
karba

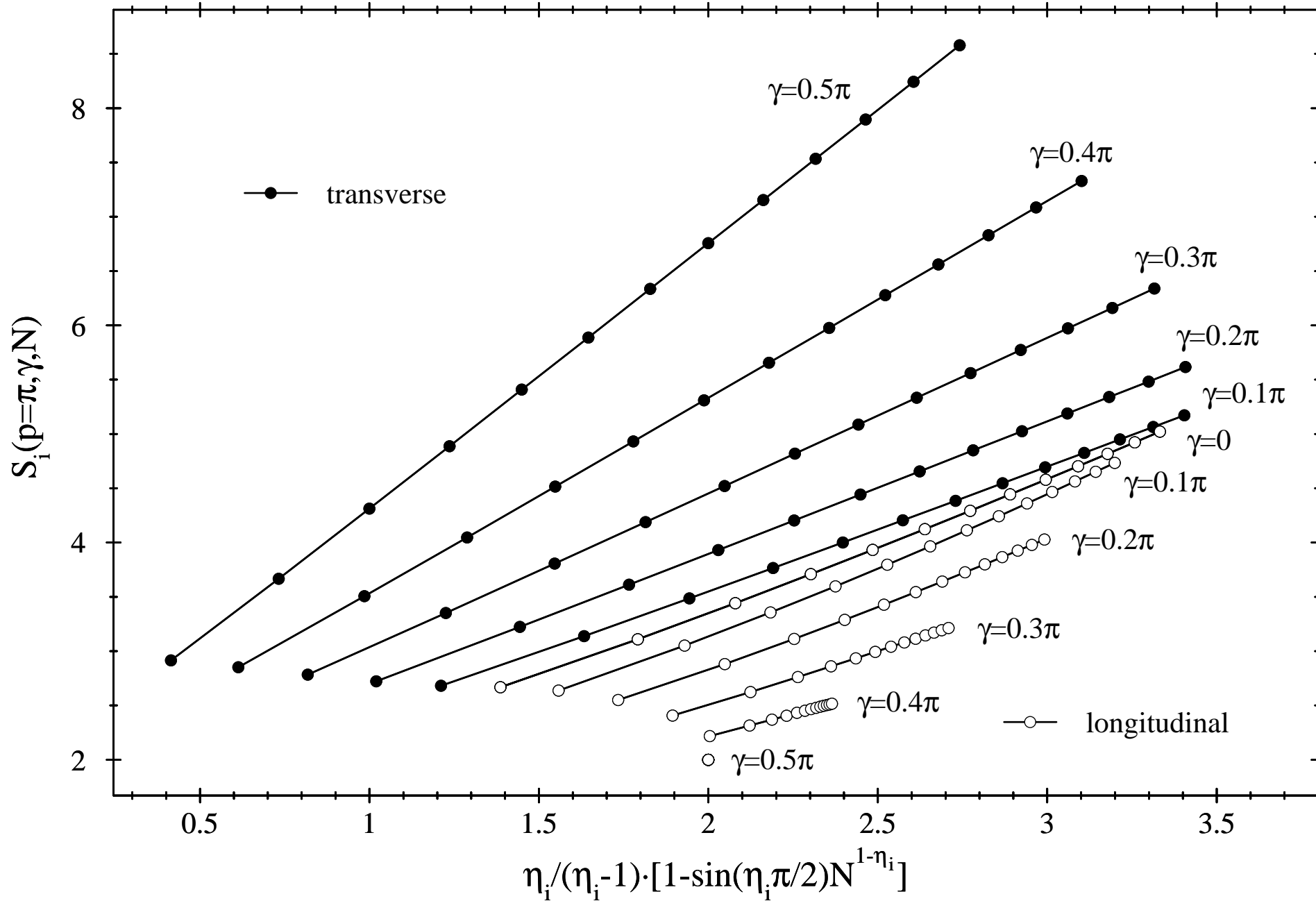


FIG. 1
karba

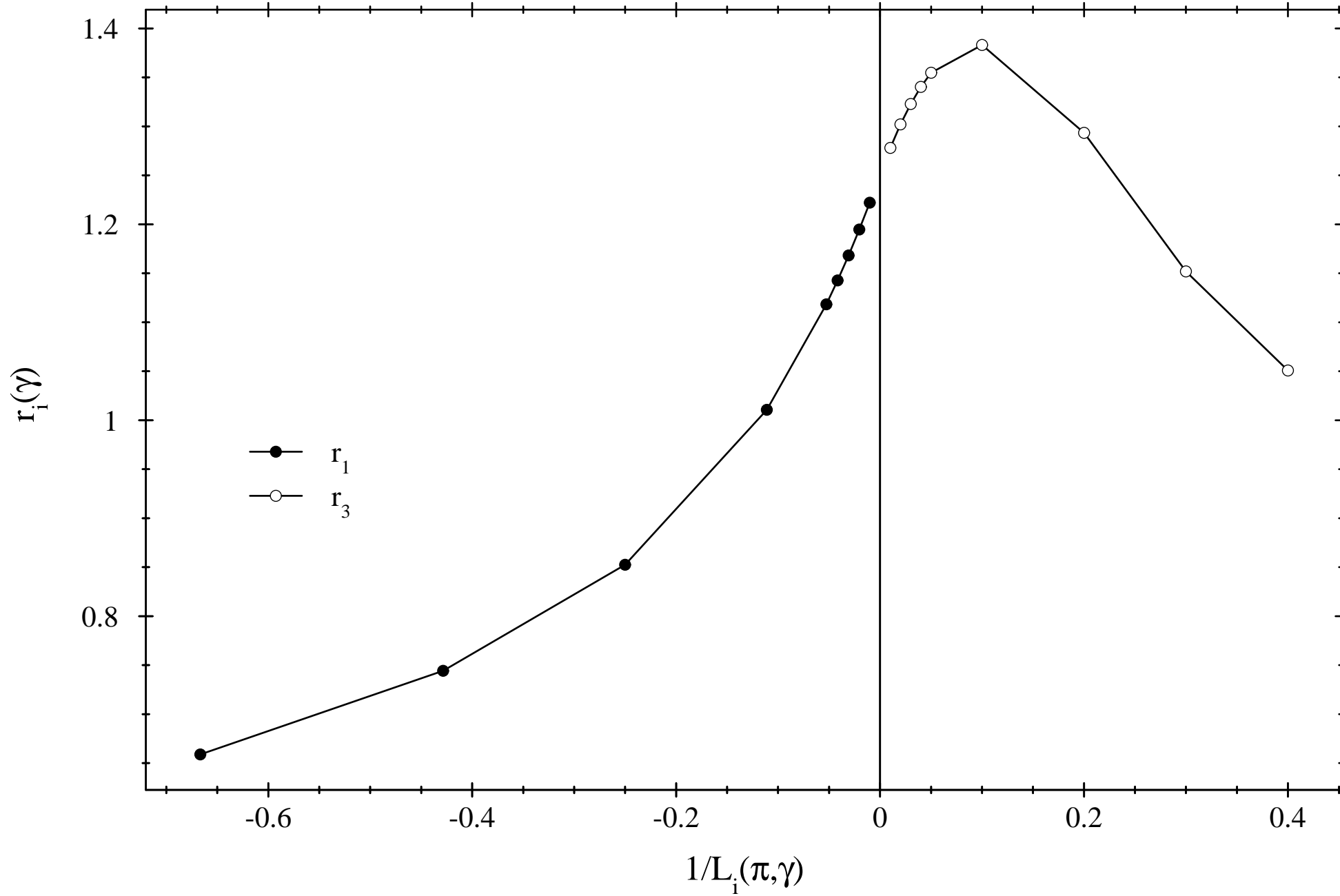


FIG.
karba

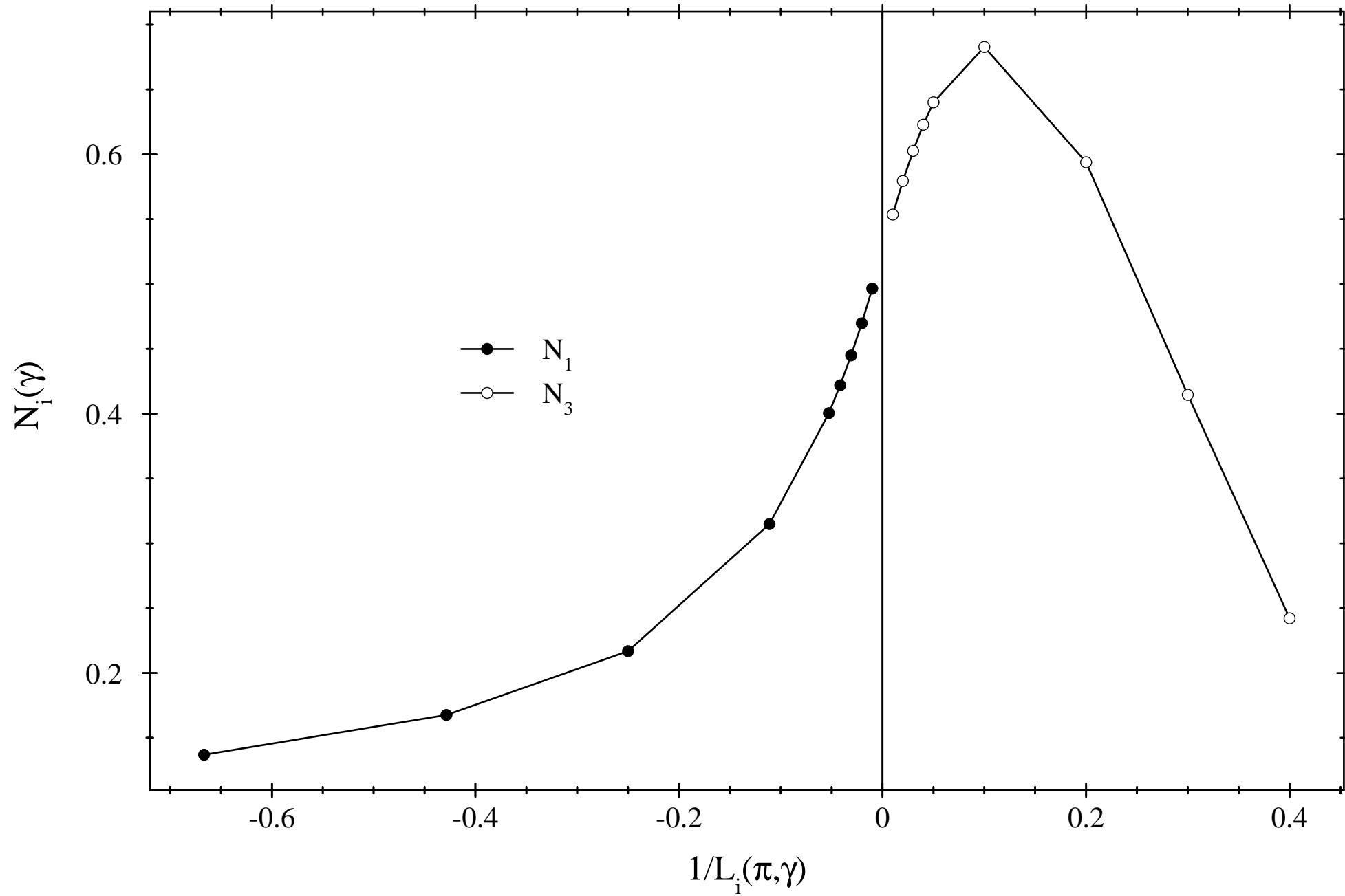


FIG.
karba